Contents lists available at ScienceDirect

Water Research X

Efficient utilization of photoelectron-hole at semiconductor-microbe interface for pyridine degradation with assistance of external electric field

Hefei Shi [a,b], Wenbo Fan [a], Xinbai Jiang [a,*], Dan Chen [a], Cheng Hou [a], Yixuan Wang [c], Yang Mu [c], Jinyou Shen [a,*]

[a] Key Laboratory of Environmental Remediation and Ecological Health, Ministry of Industry and Information Technology, School of Environmental and Biological Engineering, Nanjing University of Science and Technology, Nanjing 210094, China
[b] School of Resources and Environmental Engineering, Jiangsu University of Technology, Changzhou 213001, China
[c] CAS Key Laboratory of Urban Pollutant Conversion, Department of Environmental Science and Engineering, University of Science and Technology of China, Hefei 230026, China

ARTICLE INFO

ABSTRACT

In this study, enhanced pyridine bio-photodegradation with assistance of electricity was achieved. Meanwhile, photoelectron-hole played a vital role in accelerating pyridine biomineralization. The significant separation of photoelectron-hole was achieved with an external electric field, which provided sufficient electron donors and acceptors for pyridine biodegradation. The enhanced electron transport system activity also revealed the full utilization of photoelectron-hole by microbes at semiconductor-microbe interface with assistance of electricity. Microbial community analysis confirmed the enrichment of functional species related to pyridine biodegradation and electron transfer. Microbial function analysis and microbial co-occurrence networks analysis indicated that upregulated functional genes and positive interactions of different species were the important reasons for enhanced pyridine bio-photodegradation with external electric field. A possible mechanism of enhanced pyridine biodegradation was proposed, i.e., more photoelectrons and holes of semiconductors were utilized by microbes to accelerate reduction and oxidation of pyridine with the assistance of electrical stimulation. The excellent performance of the photoelectrical biodegradation system showed a potential alternative for recalcitrant organic wastewater treatment.

1. Introduction

Pyridine (C_5H_5N), a highly toxic environmental pollutant, has been widely found in industrial wastewater because it is common industrial raw material and solvent (Liang et al., 2018; Chen et al., 2021). Serious persistent ecological pollution would occur if untreated pyridine wastewater is discharged into the natural environment, because of the refractory, carcinogenic, teratogenic, and mutagenic properties of pyridine (Wang et al., 2018). Thus, developing economical, efficient, and eco-friendly pyridine treatment technology is of great significance to environmental protection and ecological restoration.

Biological treatment is the most used industrial wastewater treatment technology due to its economic characteristics, and has been reported to be used in pyridine removal (Niu et al., 2023; Zhang et al., 2021a). Previous studies have reported that electron acceptor was the critical factor for pyridine biodegradation (Wang et al., 2018; Hou et al.,

2018), and our previous study also reported that enhanced pyridine biodegradation was achieved with photoholes as electron acceptors at semiconductor-microbe interface (Shi et al., 2020). Besides, an interesting finding was also found, i.e., photoelectrons as electron donors could accelerate initial degradation of pyridine. Previous studies also reported the positive effect of electron donors on pyridine biodegradation (Zhang et al., 2014; Jiang et al., 2018). It is well known that electron donors and acceptors are essential for biological metabolism and pyridine degradation, and light-excited semiconductor is an ideal electron donor/acceptor source (cheap, low-energy, and sustainable) for enhancing biodegradation. However, the recombination of photoelectron-hole resulted in limited pyridine biodegradation (insufficient electron donors and acceptors). Obviously, separation efficiency of photoelectron-hole has been the key factor affecting pyridine bio-photodegradation of semiconductor-microbe interface.

Applying voltage is an effective method to accelerate the separation

of photoelectron-hole, and photoelectrocatalytic degradation was deemed to be an excellent method for eliminating organics from aqueous solutions (Gong et al., 2023; Zhang et al., 2023). As indicated by Jia et al. (2023), the efficient separation of the photoelectrons and holes at photoanode was achieved with 0.1 V anodic bias voltage was applied, resulting in excellent tetracycline degradation performance (85.6 %), which was superior to photocatalytic degradation (6.6 %). Previous studies have also proved that enhanced biodegradation has been achieved in photoelectrical biosystem (Xu et al., 2023; Guan et al., 2023). Therefore, bio-photodegradation with electrical assistance would be promising to enhance pyridine degradation. However, the mechanism of photoelectron-hole as electron donor and acceptor to enhance pyridine biodegradation has not been clarified. The role of electrical assistance on microbial metabolism of semiconductor-microbe interface has not yet been explored clearly.

In this study, BiVO₄/FeOOH, one visible light responsive semiconductor with nontoxicity, high catalytic activity, stability and biocompatibility was chosen as the photoelectrode material. The importance of photoelectron-hole for enhanced pyridine biodegradation and the pathways of pyridine bio-photodegradation with assistance of electricity was investigated. The effects of external electric field on microbial community and interactions between different microbes were discussed. Based on the reactive species trapping experiments and microbial function analysis, a possible mechanism for enhanced pyridine bio-photodegradation with electrical assistance was proposed.

2. Results and discussion

2.1. Performance of pyridine bio-photodegradation with assistance of electricity

The BiVO₄/FeOOH@CP electrode used in pyridine bio-photodegradation with assistance of electricity was characterized as in SI (Txt S1 and Figs. S1–3). The performance of 200 mg L^{-1} pyridine degradation was indicated in Fig. 1a. The biodegradation (R_{bio}) performance was negligible, and pyridine removal efficiency was only 13.79±0.78 % after 24 h, which showed the recalcitrance of pyridine for biodegradation (Shi et al., 2020). The pyridine removal performance of $R_{bio-ele}$ (biodegradation with assistance of electricity) was comparable with that of R_{bio}, which indicated the inefficient pyridine biodegradation with 0.2 V electrical stimulation. However, the degradation performance of $R_{bio-pho}$ (bio-photodegradation) was increased obviously, in comparison with R_{bio} and $R_{bio-ele}$. The pyridine removal in $R_{bio-pho}$ was 21.02±3.80 % at 12 h and eventually reached 32.18±4.83 % at 24 h. The enhanced pyridine removal could be due to that semiconductor provided electron donors/acceptors (i.e., photoelectron-hole) for microbes to degrade pyridine (Shi et al., 2020). Interesting, more significant degradation performance (65.55±2.57 % pyridine removal at 24 h) was achieved in $R_{bio-pho-ele}$ (bio-photodegradation with assistance of electricity), which was far superior to others. This result could be attributed to the efficient separation of photoelectron-hole with the assistance of electricity, which provided more electron donors and acceptors for accelerating biodegradation. Furthermore, LED lights and external electric field could be replaced by sunlight and solar panel in
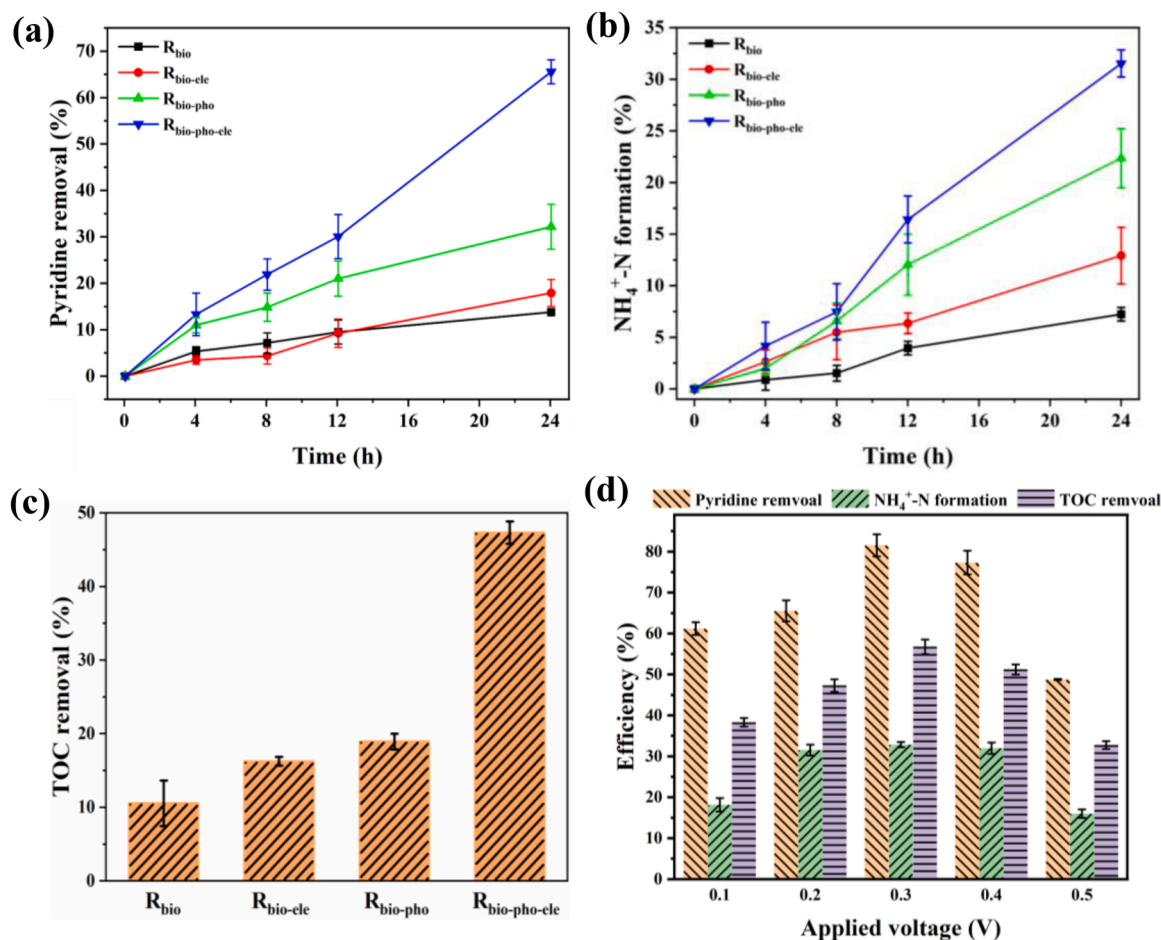
Fig. 1. Pyridine degradation (a), NH₄⁺ formation (b) and TOC removal (c) efficiency of R_{bio}, $R_{bio-ele}$, $R_{bio-pho}$ and $R_{bio-pho-ele}$; effects of applied voltage (d) on degradation performance of $R_{bio-pho-ele}$.

the future practical application, which would substantially reduce energy consumption.

NH_4^+-N (important pyridine biodegradation product) was the key evidence to evaluate the degradation performance of bioreactors (Wang et al., 2018). As indicated in Fig. 1b, NH_4^+-N formation of R_{bio} and $R_{bio-ele}$ was only 7.23±0.66 % and 12.91±2.74 % at 24 h, respectively, which was consistent with the poor pyridine removal. It was worth noting that

NH_4^+-N formation of $R_{bio-pho}$ and $R_{bio-pho-ele}$ (22.35±2.86 % and 31.52 ±1.31 %) were superior to R_{bio} and $R_{bio-ele}$, which revealed that photoelectron-hole played an essential role in accelerating pyridine biodegradation. The better NH_4^+-N formation of $R_{bio-pho-ele}$ indicated that electrical assistance could further enhance the degradation performance at semiconductor-microbe interface. TOC removal efficiencies showed similar trends to pyridine removal and NH_4^+-N formation profile
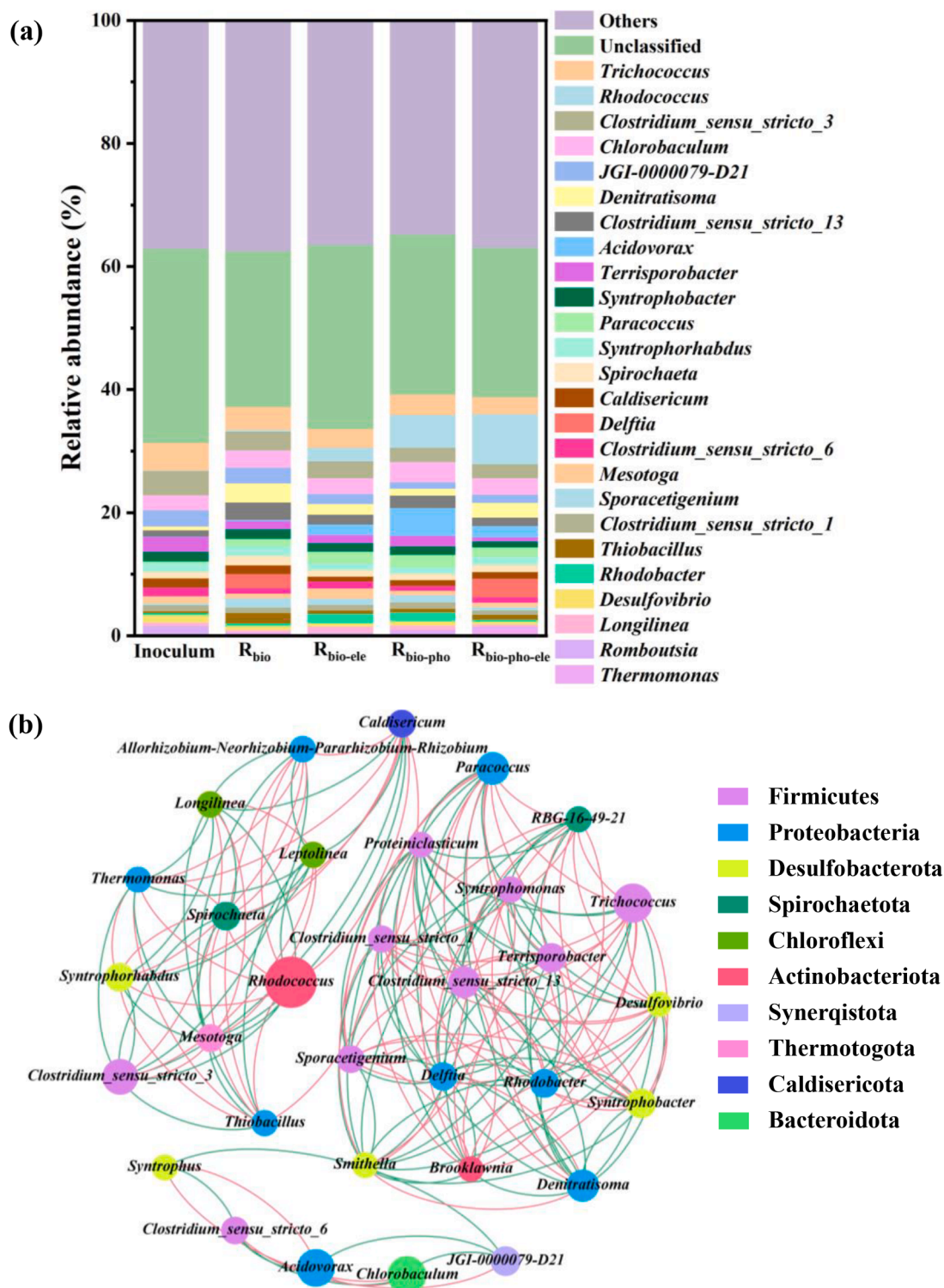
Fig. 2. Classification of microbes in different reactors at genera level (a); Co-occurrence network on genus level of the $R_{bio-pho-ele}$ (b). (The node size indicates total microbial abundance in all samples; the node color indicates phyla level of species; red color of edges shows positive relationship and green edge color shows negative relationship).

(Fig. 1c). TOC removal efficiencies of R_{bio}, $R_{bio-ele}$, $R_{bio-pho}$ and $R_{bio-pho-ele}$ were 10.52±3.11 %, 16.23±0.58 %, 18.92±1.07 % and 47.30±1.54 %, respectively. It's worth noting that there is little difference between the TOC removal efficiencies of $R_{bio-ele}$ and $R_{bio-pho}$, but $R_{bio-pho-ele}$ showed superior TOC removal performance, which suggested that electrical assistance could effectively enhance mineralization performance of semiconductor-microbe interface.

Applied voltage is an important parameter that affects both photoelectron-hole separation and microbial activity (Shi et al., 2022a; Chen et al., 2019a), which further affect pyridine degradation. In Fig. 1d, with the increase of applied voltage from 0.1 V to 0.3 V, pyridine removal and TOC removal efficiencies increased from 61.2 ± 1.57 % and 38.32±1.02 % to 81.55±2.72 % and 56.76±1.78 %, respectively. This phenomenon could be due to the higher voltage enhancing the separation of photoelectron-hole, which help provide more electron donors and acceptors for enhancing pyridine biodegradation. Besides, the higher voltage also could accelerate mass transfer velocity of substances with charges to enhance microbial metabolism (Wang et al., 2021). However, pyridine removal and TOC removal efficiencies decreased slightly to 77.33±2.89 % and 51.22±1.22 % when applied voltage further increased to 0.4 V. Moreover, pyridine removal and TOC removal efficiencies of $R_{bio-pho-ele}$ were only 48.77±0.14 % and 32.76±0.94 % with 0.5 V applied voltage, which could be due to the negative effect of high voltage on microbial activity (Safavi and Unnthorsson, 2018). NH_4^+-N formation showed a similar trend to pyridine removal and TOC removal, and it was worth noting that NH_4^+-N formation was almost unchanged with a range from 0.2 to 0.4 V. This phenomenon implied that NH_4^+-N formation might occur at a later stage of microbial metabolism, and photoelectron-hole could be preferentially used for other microbial metabolism. In short, an appropriate voltage is key for photoelectron-hole separation and microbial metabolism. The effects of other key operational parameters (acetate dosage, initial pyridine concentration and light intensity) on pyridine degradation were discussed in SI (Fig. S4–5 and Txt S2). The results revealed that acetate dosage as electron donor could accelerate pyridine degradation but excess acetate had negative effect on pyridine degradation. Poor pyridine degradation efficiency with high pyridine concentration increasing could be due to the negative effect of insufficient photoelectron-hole. The enhanced pyridine degradation with higher light intensity also revealed the importance of sufficient photoelectron-hole.

2.2. Response of microbial community at semiconductor-microbe interface with assistance of electricity

The microbial community structure of $R_{bio-pho-ele}$ has been changed obviously as compared with other reactors (Fig. S6 and Txt S3), which could be due to the selection of specific functional species with photoelectrical stimulation. At the genus level, 26 most abundant genera in five samples were analyzed. As displayed in Fig. 2a, *Trichococcus* (4.45 %), *Clostridium_sensu_stricto_3* (3.91 %) and *JGI-0,000,079-D21* (2.64 %) were found to be the dominant species in initial inoculum. *Trichococcus* (3.71 %), *Denitratisoma* (3.09 %) and *Chlorobaculum* (2.86 %) were the most dominant in R_{bio}. In $R_{bio-ele}$, *Trichococcus* (3.04 %), *Chlorobaculum* (2.61 %) and *Paracoccus* (1.92 %) were found to be the dominant species. *Rhodococcus* (5.33 %), *Trichococcus* (3.30 %) and *Chlorobaculum* (3.29 %) were most dominant in $R_{bio-pho}$. The relative abundance of *Rhodococcus* (8.15 %), *Delftia* (3.04 %) and *Trichococcus* (2.78 %) in $R_{bio-pho-ele}$ was highest.

Trichococcus was the dominant species in all samples, and *Trichococcus* has been reported to be capable of degrading various refractory organic compounds in bioreactors (Sun et al., 2013; Guo et al., 2014). Besides, *Trichococcus* was also found to be an electroactive species that can directly or indirectly accept electrons (Chen et al., 2019b). The excellent ability of degradation and electron transfer could be important reasons that be responsible for the dominant position of *Trichococcus* in all reactors. *Chlorobaculum*, a dominant species in R_{bio}, $R_{bio-ele}$ and

$R_{bio-pho}$, was found to play a crucial role in toxic organic matter degradation in a bioelectrochemical system (Zhang et al., 2016). *Denitratisoma* dominated in R_{bio} and has been reported to play a vital role in anaerobic organic matter degradation (Chiang et al., 2020). *Paracoccus* was found to be a good pyridine degrader in previous studies (Shen et al., 2015; Wang et al., 2018), and the increased relative abundance of *Paracoccus* in $R_{bio-ele}$ was probably due to the direct stress by pyridine. According to previous studies (Shi et al., 2022a; Hou et al., 2018), *Rhodococcus* not only had excellent pyridine degradation ability but also was an efficient electroactive species. In comparison to inoculum, the relative abundance of *Rhodococcus* in $R_{bio-pho}$ and increased obviously, which could be due to that the utilization of photoelectron-hole accelerated the growth of *Rhodococcus*. Notably, the relative abundance of *Rhodococcus* further increased in $R_{bio-pho-ele}$, indicating that assistance of electricity created more favorable conditions for *Rhodococcus* growth and enhanced pyridine bio-photodegradation. In the study of Zheng et al. (2022), *Delftia* was the dominant species in membrane-aerated biofilm reactor and played a crucial role in high load pyridine degradation. In addition, *Delftia* has been found to be dominant species in several bioelectrochemical systems because of its outstanding electron transfer capability (Feng et al., 2017; Sun et al., 2016). In conclusion, above results suggested the vital role of electricity for enriching functional species at semiconductor-microbe interface.

The co-occurrence network (contained 170 edges among 31 nodes; degree centrality and closeness centrality≥ 0.21) at genus level as shown in Fig. 2b, revealing the complex interactions between functional species (Zhang et al., 2021b). A significant positive interaction could be observed between *Rhodococcus* and *Thermomonas* ($r = 1.0, p< 0.05$), and *Thermomonas* has been reported as an excellent pyridine degrader (Xu et al., 2020). A similar symbiotic relationship could be found between *Rhodococcus* and *Thiobacillus* ($r = 1.0, p< 0.05$), notably, *Thiobacillus* (typical electroactive species) was found to be a dominant species in photoelectrical biodegradation system (Chen et al., 2020; Zhao et al., 2023). The relative abundances of *Thermomonas* and *Thiobacillus* in $R_{bio-pho-ele}$ (1.26 % and 0.80 %) were significantly higher than $R_{bio-pho}$ (0.37 % and 0.61 %), and the positive interactions of *Thermomonas* and *Thiobacillus* with *Rhodococcus* might result in excellent pyridine degradation in $R_{bio-pho-ele}$. It was interesting to note that *Paracoccus* and *Delftia* (core species of $R_{bio-pho-ele}$) were significantly negatively correlated ($r= -1.0, p< 0.05$), and relative abundance of *Paracoccus* in $R_{bio-pho-ele}$ (1.51 %) decreased obviously as compared with $R_{bio-pho}$ (1.99 %). Above results implied that electrical assistance could achieve efficient optimization of microbial community structure at semiconductor-microbe interface.

In short, the pyridine biodegradation species (*Rhodococcus, Trichococcus, Delftia, Thermomonas* and *Thiobacillus*) and electroactive species (*Rhodococcus, Trichococcus, Delftia* and *Thiobacillus*) could be well enriched in $R_{bio-pho-ele}$ with photoelectrical stimulation. The enrichment of functional species and the positive interactions of them were the important reasons for enhanced pyridine bio-photodegradation with external electric field.

2.3. Microbial function analysis

Hydroxylation was the initial reaction of aerobic pyridine biodegradation (Wang et al., 2018), and our previous study has also found that nicotinate dehydrogenase and 6-hydroxynicotinate 3-monooxygenase were the key functional enzymes for hydroxylation of pyridine (Zheng et al., 2022). However, the gene (*nicA/C*) abundance of the above two functional enzymes was unobvious according to PICRUSt2 (Fig. 3), which could be due to the insufficient dissolved oxygen in $R_{bio-pho-ele}$. Notably, the encoding gene of pteridine reductase (*PTR1*), a functional enzyme for the reduction of nitrogenous heterocyclic compounds (Nare et al., 1997), increased obviously in $R_{bio-pho-ele}$, which was consistent with the result of pyridine degradation process (production of piperidine; Fig. S7–8, Table S2 and Txt S4 in SI). Flavin-dependent
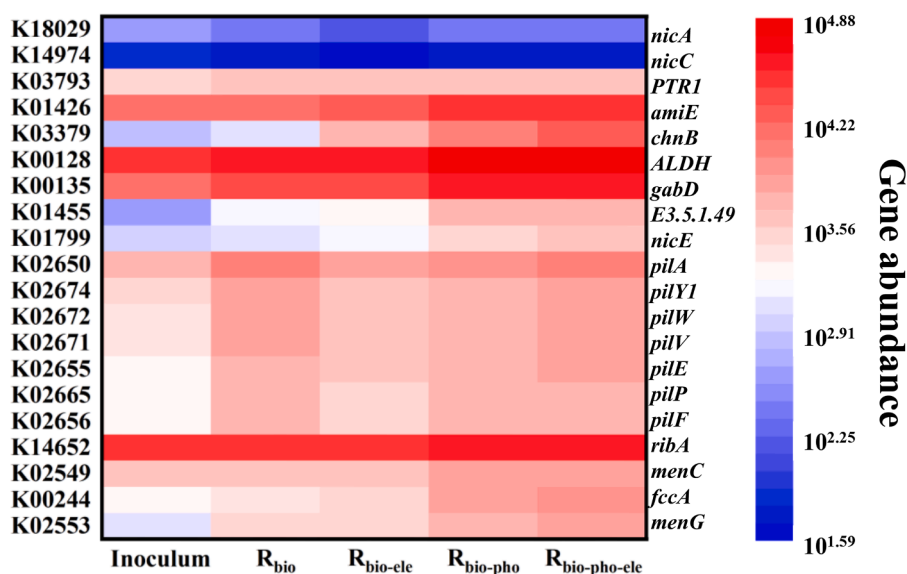
Fig. 3. Pyridine biodegradation and extracellular electron transfer related functions predicted from the 16S rRNA gene-based microbial compositions using PICRUSt2 algorithm.

monooxygenase played a key role for pyridine ring cleavage (Čašaitė et al., 2020), and increased abundance of gene *chnB* (encoding cyclohexanone monooxygenase, a typical flavin-dependent monooxygenase) was observed in $R_{bio\text{-}pho\text{-}ele}$, which could contribute to the further degradation and ring cleavage of piperidine. Furthermore, amidase, aldehyde dehydrogenase, semialdehyde dehydrogenase, formamidase and maleate isomerase (encoded by *amiE, ALDH, gabD, E3.5.1.49* and *nicE*) involved the subsequent pyridine degradation, and the abundance of these genes upregulated markedly in $R_{bio\text{-}pho\text{-}ele}$. The increased abundance of functional genes related to pyridine degradation was consistent with the excellent performance of $R_{bio\text{-}pho\text{-}ele}$, revealing the positive impact of electrical assistance on pyridine bio-photodegradation.

The process of pyridine biodegradation is essentially the gain and loss of electrons under biocatalysis, thus, electron transfer is a crucial factor that affects pyridine degradation. It is well-known that direct and indirect electron transfer are two main microbial extracellular electron transfer pathways (Zhang et al., 2019). Outer membrane c-type cytochromes (encoded by *fccA*) and electro-conductive pilin (*PilA/E/F/P/V/W/Y1*) were the important methods for microbes to direct electron transfer. Genes *menC/G* and *ribA* were involved in the intermediates biosyntheses of these soluble electron shuttles, which played a crucial role in indirect electron transfer (Pang and Wang, 2020). According to PICRUSt2 results, upregulation of these genes was observed in $R_{bio\text{-}pho\text{-}ele}$, indicating that photoelectron-hole were utilized as electron donor/acceptor, and both direct and indirect electron transfer were accelerated in $R_{bio\text{-}pho\text{-}ele}$.

2.4. Mechanism for pyridine bio-photodegradation with assistance of electricity

As shown in Fig. 4 and SI (Fig S9 and Txt S5), ETS activity and EPS activity of $R_{bio\text{-}pho\text{-}ele}$ has increased obviously, which could be due to the positive effect of electrical assistance on microbial electron transfer and pyridine bio-photodegradation. Besides, •OH and photohole were the main reaction species in $R_{bio\text{-}pho\text{-}ele}$, and photohole played a more important role in pyridine biodegradation. According to the above analysis, a possible mechanism for enhanced pyridine bio-photodegradation with electrical assistance was proposed. As displayed in Fig. 5, $BiVO_4/FeOOH$ semiconductors were excited under visible light irradiation with the generation of photoelectron-hole, and

the effective separation of photoelectron-hole could be achieved with the external electric field. Although a part of pyridine was degraded by photohole and •OH, more pyridine was reduced to piperidine by cathodic microbes with utilizing photoelectrons, which was revealed by pyridine degradation pathway. This could reduce the toxicity and refractoriness of pyridine and facilitate biomineralization, which was consistent with the positive role of electron donors for pyridine biodegradation in previous studies (Xu et al., 2017; Zhang et al., 2014). Piperidine and other intermediates were further degraded until mineralization by microbes with the assistance of photoholes, and Ye et al. (2022) also found that photoholes could accelerate the degradation of organics in a light-driven biohybrid system. Photohole, the main reactive species in $R_{bio\text{-}pho\text{-}ele}$, played a crucial role in enhanced pyridine degradation, especially in biomineralization. Our previous studies have reported the importance of electron acceptors in pyridine biodegradation (Shen et al., 2015; Hou et al., 2018), and a similar result was achieved by photoholes in this study. ETS activity, EPS and EEM results indicated enhanced extracellular electron transfer in $R_{bio\text{-}pho\text{-}ele}$, revealing the efficient utilization of photoelectron-hole by microbes. Microbial community analysis showed that pyridine biodegradation species and electroactive species were enriched in $R_{bio\text{-}pho\text{-}ele}$, indicating the positive evolution of microbial community with photoelectrical stimulation. Pyridine degradation intermediates were further degraded until mineralization by degradation functional species, and electrons produced during biodegradation were accepted by photoholes with the assistance of electroactive species. The abundance of functional gene (related to pyridine degradation and electron transfer) was also increased according to PICRUSt2 results, which could be one of important reasons for excellent performance in $R_{bio\text{-}pho\text{-}ele}$. Thus, efficient photoelectron-hole separation was achieved with external electric field resulting more electron donors and acceptors were utilized by microbes for pyridine degradation, which showed the great potential of $R_{bio\text{-}pho\text{-}ele}$ system in refractory organic wastewater treatment.

3. Conclusions

In this study, enhanced pyridine bio-photodegradation with electrical assistance was successfully achieved. The recombination of photoelectron-hole was inhibited effectively with external electric field, which provided sufficient electron donor and acceptor for pyridine biodegradation. The calculated maximum pyridine removal rate in $R_{bio\text{-}}$
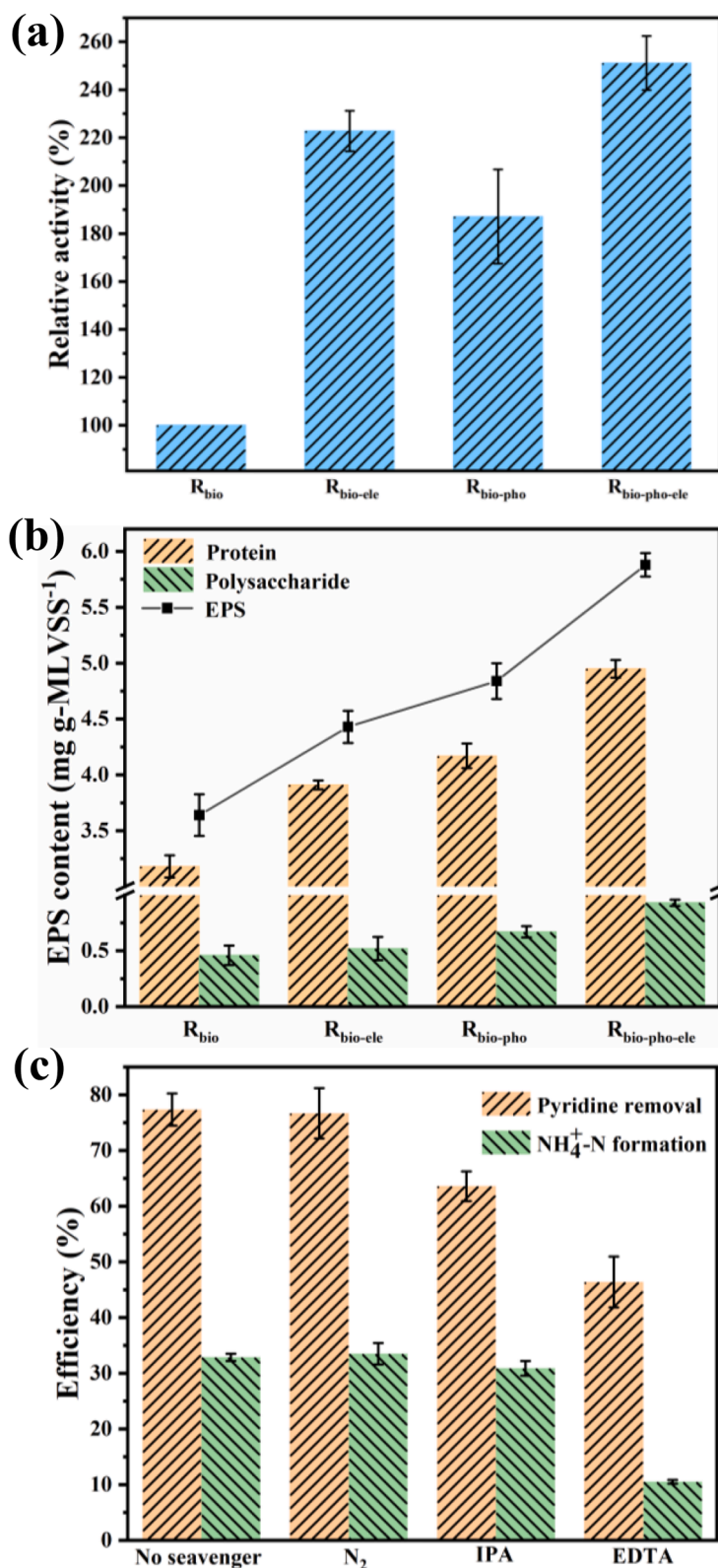
Fig. 4. ETS (a) and EPS activity (b) of different reactors; effect of scavengers on pyridine removal and ammonia formation in $R_{bio-pho-ele}$ (c).

$_{pho-ele}$ was 5.06 mol $m^{-3} \cdot d^{-1}$, which was 2.16 times of that in our previous bio-photodegradation system (Shi et al., 2020), indicating the importance of electrical assistance for semiconductor-microbe interface. The upregulated functional genes (related to electron transfer and pyridine degradation) and the positive interactions of different species played a key role in enhancing degradation performance of $R_{bio-pho-ele}$

according to the results of PICRUSt2 and co-occurrence network analysis, and a possible mechanism for enhanced pyridine biodegradation was proposed. Semiconductor-microbe interface with electrical assistance provides a promising and feasible alternative for recalcitrant organic wastewater treatment.
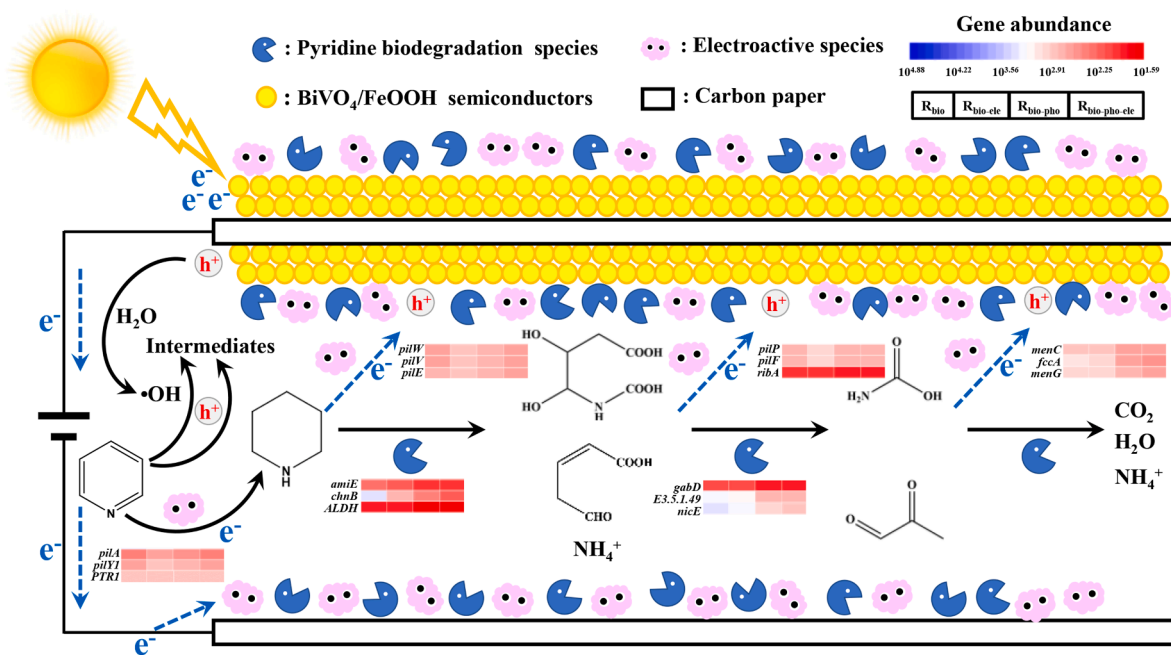
Fig. 5. Possible mechanism of pyridine biodegradation in $R_{bio-pho-ele}$.

4. Materials and methods

4.1. Materials and synthesis of photoanode

All reagents used in this study were of analytical grade (purity > 99.9 %) and used without further purification. Carbon paper (CP) purchased from Toray Co. (Japan) was sonicated and then dried to remove impurities before use, and BiVO₄/FeOOH@CP indicated in our previous study was used as photoanode in this study (Shi et al., 2020) (SI, Txt S6).

4.2. Reactor set up and operation

Cuboid plexiglass reactor with cylindrical hollow structure (φ100 mm × 30 mm, effective volume of 220 mL) were used in this study, and one side of the reactor is made of quartz glass to allow the semiconductor in reactor to absorb visible light (Fig. S10). BiVO₄/FeOOH@CP and blank CP were used as photoanode and cathode, respectively. A LED lamp provided the light for reactor and a regulated DC power source (PS-302D-2, Shenzhen Zhaoxin Electronic Co. LTD., China) was used to control voltage difference between electrodes and Ag/AgCl electrode (assumed + 0.197 V vs. SHE) was used as a reference. The seed sludge was collected from a bioreactor treating pyridine-containing wastewater. The initial concentration of mixed liquor suspended solids (MLSS) in reactor was approximately 3.0 g L⁻¹, and then reactors were operated in batch mode (24 h) with synthetic wastewater. The supernatant was drained off after 24 h and one new batch was started by adding fresh synthetic wastewater. The system reached a steady state after 30 days, and biofilm was enriched onto electrodes. The photoelectrode always remained stable during the start-up phase. The composition of synthetic wastewater was as follows: phosphate buffer (7 mM, pH=7.0), MgSO₄·7H₂O (0.2 g·L⁻¹), CaCl₂ (0.05 g·L⁻¹), pyridine at desired concentration and trace element solution (1 mL·L⁻¹) (Shi et al., 2020), and pyridine was the only carbon and nitrogen sources for microbes in this study.

In order to verify the positive role of electricity for pyridine bio-photodegradation, four reactors were operated in parallel at 35±2 °C in a greenhouse. The reactor operated in an open circuit with biomass and blank CP as both anode and cathode, was named after R_{bio}. The reactor operated in a closed circuit (0.2 V) with biomass and blank CP as

both anode and cathode, was named after $R_{bio-ele}$. The reactor operated in an open circuit with biomass and BiVO₄/FeOOH@CP as anode and blank CP as cathode, was named after $R_{bio-pho}$. The reactor operated in a closed circuit (0.2 V) with biomass and BiVO₄/FeOOH@CP as anode and blank CP as cathode, was named after $R_{bio-pho-ele}$. All reactors used a 100 W LED lamp as a visible light source with a light density meter (1919-R, Newport, USA) measuring and adjusting light intensity. Several key operational parameters including applied voltage, acetate dosage, initial pyridine concentration and light intensity were investigated in this study (Table S3). Different scavengers could inhibit and block corresponding reactive oxidative species (ROS), providing powerful evidences to identify the role of different ROS in pyridine degradation. In order to find the main ROS responsible for pyridine degradation, 10 mM isopropanol (IPA) for hydroxyl radical ($\bullet OH$), 30 min nitrogen purging for superoxide radical ($\bullet O_2^-$), and 10 mM ethylenediaminetetraacetic acid (EDTA) for photoholes (h^+) (Shi et al., 2022a, 2022b).

4.3. Analytic methods

The prepared BiVO₄/FeOOH@CP was characterized by field emission scanning electron microscopy (FE-SEM, Quant 250FEG, FEI, USA), X-ray diffraction (XRD, D8 Advance, Bruker, Germany) and X-ray photoelectron spectroscopy (XPS, ESCALAB 250, Thermo, USA). All the photochemical tests were characterized by a potentiostat (VMP3, Bio-Logic Science Instruments, France) and a 300 W Xe lamp. The photocurrent response and electrochemical impedance spectroscopy (EIS) analysis were measured according to our previous study (Shi et al., 2022a) (SI, Txt S6). Pyridine degradation performance was evaluated by High performance liquid chromatography (HPLC, UltiMate 3000, Thermo, USA) and a total organic carbon (TOC) analyzer (vario TOC, Elementar, Germany). NH_4^+-N, NO_2^--N and NO_3^--N were also measured according to Hou et al. (2018), and NO_2^--N and NO_3^--N were undetectable.

Three-dimensional fluorescence excitation-emission matrix (3D-EEM) analysis and HPLC/MS were used in the analysis of soluble microbial products and pyridine degradation intermediates (Shi et al., 2020). Extracellular polymeric substances (EPS) were extracted using a Na⁺-form cation exchange resin, and the protein (PN) and polysaccharide (PS) contents in the extracted EPS were quantified using the

Lowry and Anthrone methods, respectively, according to Zhang et al. (2020). Electron transport system (ETS) activity was performed to assess the microbial activity and electron transfer of biodegradation system (Xia et al., 2022) (SI, Txt S6). The microbial community structure of inoculum, R_{bio}, $R_{bio-ele}$ $R_{bio-pho}$ and $R_{bio-pho-ele}$ were profiled using high-throughput sequencing technology, according to Jiang et al. (2018). Moreover, Phylogenetic Investigation of Communities by Reconstruction of Unobserved States 2 (PICRUSt2) was used to predict the functional potential of the microbial community according to the Kyoto Encyclopedia of Genes and Genomes (KEGG) database (Douglas et al., 2020).

CRediT authorship contribution statement

Hefei Shi: Writing – original draft, Visualization, Investigation, Data curation. **Wenbo Fan:** Visualization. **Xinbai Jiang:** Writing – review & editing, Funding acquisition. **Dan Chen:** Visualization. **Cheng Hou:** Data curation. **Yixuan Wang:** Visualization. **Yang Mu:** Writing – review & editing. **Jinyou Shen:** Writing – review & editing, Project administration, Funding acquisition, Conceptualization.

Declaration of competing interest

The authors declare that they have no known competing financial interests or personal relationships that could have appeared to influence the work reported in this paper.

Data availability

Data will be made available on request.

Acknowledgments

Supplementary materials

Supplementary material associated with this article can be found, in the online version, at doi:10.1016/j.wroa.2024.100214.

References

Časaitė, V., Stanislauskienė, R., Vaitekūnas, J., Tauraitė, D., Rutkienė, R., Gasparavičiūtė, R., Meškys, R., 2020. Microbial degradation of pyridine: a complete pathway in *Arthrobacter sp. Strain 68b Deciphered*. Appl. Environ. Microb. 86, e00902–e00920.

Chen, D., Shen, J., Jiang, X., Su, G., Han, W., Sun, X., Li, J., Mu, Y., Wang, L., 2019a. Simultaneous debromination and mineralization of bromophenol in an up-flow electricity-stimulated anaerobic system. Water Res. 157, 8–18.

Chen, X., Xu, Y., Fan, M., Chen, Y., Shen, S., 2019b. The stimulatory effect of humic acid on the co-metabolic biodegradation of tetrabromobisphenol A in bioelectrochemical system. J. Environ. Manag. 235, 350–356.

Chen, M., Zhou, X., Chen, X., Cai, Q., Zeng, R., Zhou, S., 2020. Mechanisms of nitrous oxide emission during photoelectrotrophic denitrification by self-photosensitized *Thiobacillus denitrificans*. Water Res. 172, 115501.

Chen, D., Zhang, X., Chen, H., Shi, H., Jiang, X., Mu, Y., Pant, D., Han, W., Sun, X., Li, J., Shen, J., Wang, L., 2021. Simultaneous removal of pyridine and denitrification in an integrated bioelectro-photocatalytic system utilizing N-doped graphene/α-Fe$_2$O$_3$ modified photoanode. Electrochim. Acta 366, 137425.

Chiang, Y., Wei, S., Wang, P., Wu, P., Yu, C., 2020. Microbial degradation of steroid sex hormones: implications for environmental and ecological studies. Microb. Biotechnol. 13, 926–949.

Douglas, G., Maffei, V., Zaneveld, J., Yurgel, S., Brown, J., Taylor, C., Huttenhower, C., Langille, M., 2020. PICRUSt2 for prediction of metagenome functions. Nat. Biotechnol. 38, 685–688.

Feng, Y., Li, X., Song, T., Yu, Y., Qi, J., 2017. Stimulation effect of electric current density (ECD) on microbial community of a three dimensional particle electrode coupled with biological aerated filter reactor (TDE-BAF). Bioresour. Technol. 243, 667–675.

Gong, Y., Wang, J., Cheng, Z., Han, Z., Zhao, X., Chai, B., Han, Y., 2023. Developing high-quality g-C$_3$N$_4$ film electrode for the photoelectrocatalytic degradation of methylene blue in water. Chinese Chem. Lett. 34, 107535.

Guan, J., Gao, X., Yuan, Y., Wang, C., An, R., Lu, P., Lu, N., 2023. Synergic mechanisms of electricity generation and bisphenol a degradation in a novel photocatalytic-microbial fuel cell equipped with a TiO$_2$-C-BiVO$_4$ photo-anode and a biofilm-anode. Chem. Eng. J. 471, 144308.

Guo, W., Feng, J.L., Song, H., Sun, J.H., 2014. Simultaneous bioelectricity generation and decolorization of methyl orange in a two-chambered microbial fuel cell and bacterial diversity. Environ. Sci. Pollut. Res. 21, 11531–11540.

Hou, C., Shen, J., Jiang, X., Zhang, D., Sun, X., Li, J., Han, W., Liu, X., Wang, L., 2018. Enhanced anoxic biodegradation of pyridine coupled to nitrification in an inner loop anoxic/oxic-dynamic membrane bioreactor (A/O-DMBR). Bioresour. Technol. 267, 626–633.

Jia, L., Yang, C., Jin, X., Wang, D., Li, F., 2023. Direct Z-scheme heterojunction Bi/Bi$_2$S$_3$/α-MoO$_3$ photoelectrocatalytic degradation of tetracycline under visible light. Chemosphere 315, 137777.

Jiang, X., Shen, J., Xu, K., Chen, D., Mu, Y., Sun, X., Han, W., Li, J., Wang, L., 2018. Substantial enhancement of anaerobic pyridine bio-mineralization by electrical stimulation. Water Res. 130, 291–299.

Liang, J., Li, W., Zhang, H., Jiang, X., Wang, L., Liu, X., Shen, J., 2018. Coaggregation mechanism of pyridine-degrading strains for the acceleration of the aerobic granulation process. Chem. Eng. J. 338, 176–183.

Nare, B., Luba, J., Hardy, L., Beverley, S., 1997. New approaches to Leishmania chemotherapy: pteridine reductase 1 (*PTR1*) as a target and modulator of antifolate sensitivity. Parasitology 114, 101–110.

Niu, H., Nie, Z., Long, Y., Guo, J., Tan, J., Bi, J., Yang, H., 2023. Efficient pyridine biodegradation by *Stenotrophomonas maltophilia* J2: degradation performance, mechanism, and immobilized application for wastewater. J. Hazard. Mater. 459, 132220.

Pang, Y., Wang, J., 2020. Insight into the mechanism of chemoautotrophic denitrification using pyrite (FeS$_2$) as electron donor. Bioresour. Technol. 318, 124105.

Safavi, S., Unnthorsson, R., 2018. Enhanced methane production from pig slurry with pulsed electric field pre-treatment. Environ. Technol. 4, 479–489.

Shen, J., Chen, Y., Wu, S., Wu, H., Liu, X., Sun, X., Li, J., Wang, L., 2015. Enhanced pyridine biodegradation under anoxic condition: the key role of nitrate as the electron acceptor. Chem. Eng. J. 277, 140–149.

Shi, H., Jiang, X., Chen, D., Li, Y., Hou, C., Wang, L., Shen, J., 2020. BiVO$_4$/FeOOH semiconductor-microbe interface for enhanced visible-light-driven biodegradation of pyridine. Water Res. 187, 116464.

Shi, H., Chen, D., Jiang, X., Li, Y., F, W., Hou, C., Zhang, L., Wang, Y., Mu, Y., Shen, J., 2022a. Simultaneous high-concentration pyridine removal and denitrification in an electricity assisted bio-photodegradation system. Chem. Eng. J. 430, 132598.

Shi, H., Jiang, X., Li, Y., Chen, D., Hou, C., Zhang, Z., Zhang, Q., Shen, J., 2022b. Enhanced bio-photodegradation of p-chlorophenol by CdS/g-C$_3$N$_4$ 3D semiconductor-microbe interfaces. Sci. Total Environ. 807, 151006.

Sun, J., Li, Y.M., Hu, Y.Y., Hou, B., Zhang, Y.P., Li, S.Z., 2013. Understanding the degradation of Congo red and bacterial diversity in an air-cathode microbial fuel cell being evaluated for simultaneous azo dye removal from wastewater and bioelectricity generation. Appl. Microbiol. Biotechnol. 97, 3711–3719.

Sun, Q., Li, Z., Wang, Y., Yang, C., Chung, J., Wang, A., 2016. Cathodic bacterial community structure applying the different co-substrates for reductive decolorization of Alizarin Yellow R. Bioresour. Technol. 208, 64–72.

Wang, J., Jiang, X., Liu, X., Sun, X., Han, W., Li, J., Wang, L., Shen, J., 2018. Microbial degradation mechanism of pyridine by *Paracoccus* sp. NJUST30 newly isolated from aerobic granules. Chem. Eng. J. 344, 86–94.

Wang, H., Zheng, X., Yan, Q., Zhang, G., Kim, J., 2021. Microbial community and metabolic responses to electrical field intensity for alleviation of ammonia inhibition in an integrated bioelectrochemical system (BES). Bioresour. Technol. 336, 125332.

Xia, Y., Jiang, X., Wang, Y., Huang, Q., Chen, D., Hou, C., Mu, Y., Shen, J., 2022. Enhanced anaerobic reduction of nitrobenzene at high salinity by betaine acting as osmoprotectant and regulator of metabolism. Water Res. 223, 118982.

Xu, H., Sun, W., Yan, N., Li, D., Wang, X., Yu, T., Zhang, Y., Rittmann, B., 2017. Competition for electrons between pyridine and quinoline during their simultaneous biodegradation. Environ. Sci. Pollut. R. 24, 25082–25091.

Xu, W., Zhao, H., Cao, H., Zhang, Y., Sheng, Y., Li, T., Zhou, S., Li, H., 2020. New insights of enhanced anaerobic degradation of refractory pollutants in coking wastewater: role of zero-valent iron in metagenomic functions. Bioresour. Technol. 300, 122667.

Xu, Y., Liu, X., Xiang, J., Zhang, Z., Qiao, X., Li, Y., He, Q., Lü, J., 2023. Nitrogen−doped−CQDs/schwertmannites as visible−light−responsive Fenton catalysts for the degradation of chlortetracycline and related cytotoxicity. J. Clean. Prod. 391, 136245.

Ye, J., Chen, Y., Chao, G., Wang, C., Hu, A., Dong, G., Chen, Z., Zhou, S., Xiong, Y., 2022. Sustainable conversion of microplastics to methane with ultrahigh selectivity by biotic-abiotic hybrid photocatalytic system. Angew. Chem. Int. Ed. 61, e202213244.

Zhang, Y., Chang, L., Yan, N., Tang, Y., Liu, R., Rittmann, B.E., 2014. UV photolysis for accelerating pyridine biodegradation. Environ. Sci. Technol. 48, 649–655.

Zhang, L., Jiang, X., Shen, J., Xu, K., Li, J., Su, X., Han, W., Wang, L., 2016. Enhanced bioelectrochemical reduction of p-nitrophenols in the cathode of self-driven microbial fuel cells. RSC Adv. 6, 29072–29079.

Zhang, Q., Amor, K., Galer, S., Thompson, I., Porcelli, D., 2019. Using stable isotope fractionation factors to identify Cr(VI) reduction pathways: metal-mineral-microbe interactions. Water Res. 151, 98–109.

Zhang, D., Li, Y., Sun, A., Tong, S., Jiang, X., Mu, Y., Li, J., Han, W., Sun, X., Wang, L., Shen, J., 2020. Optimization of S/Fe ratio for enhanced nitrobenzene biological removal in anaerobic System amended with Sulfide-modified nanoscale zerovalent iron. Chemosphere 247, 125832.

Zhang, X., Hou, Y., Jiang, X., Chen, D., Ge, S., Wang, L., Shen, J., 2021a. Development of a Microalgal (*Chlorella*)-Bacterial (*Paracoccus*) symbiotic system for pyridine biodegradation under photosynthetic oxygenation. ACS EST Water 1, 356–365.

Zhang, H., Xu, L., Huang, T., Yan, M., Liu, K., Miao, Y., He, H., Li, S., Sekar, R., 2021b. Combined effects of seasonality and stagnation on tap water quality: changes in chemical parameters, metabolic activity and co-existence in bacterial community. J. Hazard. Mater. 403, 124018.

Zhang, X., Yu, W., Guo, Y., Li, S., Chen, Y., Wang, H., Bian, Z., 2023. Recent advances in photoelectrocatalytic advanced oxidation processes: from mechanism understanding to catalyst design and actual applications. Chem. Eng. J. 455, 140801.

Zhao, X., Huang, S., Chen, X., Zeng, R., Zhou, S., Chen, M., 2023. Mechanisms of extracellular photoelectron uptake by a *Thiobacillus denitrificans*-cadmium sulfide biosemiconductor system. Chem. Eng. J. 468, 143667.

Zheng, P., Li, Y., Chi, Q., Cheng, Y., Jiang, X., Chen, D., Mu, Y., Shen, J., 2022. Structural characteristics and microbial function of biofilm in membrane-aerated biofilm reactor for the biodegradation of volatile pyridine. J. Hazard. Mater. 437, 129370.